J Fluoresc
DOI 10.1007/s10895-014-1355-6

ORIGINAL PAPER

Synthesis, Characterization, DNA Binding, Light Switch "On and Off", Docking Studies and Cytotoxicity, of Ruthenium(II) and Cobalt(III) Polypyridyl Complexes

M. Rajender Reddy · Putta Venkat Reddy · Yata Praveen Kumar · A. Srishailam · Navaneetha Nambigari · S. Satyanarayana

Received: 22 September 2013 / Accepted: 27 January 2014

Abstract The novel ligand (dmbip) 2-(4-N, N-dimethylbenzenamine)1H-imidazo[4, 5-f][1, 10]phenanthroline and its complexes $[Ru(phen)_2dmbip]^{2+}$ (1), $[Ru(bpy)_2dmbip]^{2+}$ (2), $[Co(phen)_2dmbip]^{3+}$ (3) and $[Co(bpy)_2dmbip]^{3+}$ (4) [where phen=1, 10-phenanthroline, bpy=2, 2′-bipyridine], have been synthesized and characterized by elemental analysis, IR, UV-Vis, ^1H NMR, ^{13}C NMR and Mass spectra. The DNA binding properties of the complexes were investigated by absorption, emission, quenching studies, light switch "on and off", salt dependent, sensor (cation and anion) studies, viscosity measurements, cyclic voltammetry, molecular modeling and docking studies. The four complexes were screened for Photo cleavage of pBR322 DNA, antimicrobial activity and cytotoxicity. The experimental results indicate that the four complexes can intercalate into DNA base pairs. The DNA-binding affinities of these complexes follow the order $[Ru(phen)_2dmbip]^{2+} > [Co(phen)_2dmbip]^{3+} > [Ru(bpy)_2dmbip]^{2+} > [Co(bpy)_2dmbip]^{3+}$.

Keywords Ru(II) & Co(III) complexes · Calf thymus DNA · Photocleavage · Antimicrobial activity · Sensors · Cyclic voltammetry · Cytotoxicity

M. R. Reddy · P. V. Reddy · Y. P. Kumar · A. Srishailam · S. Satyanarayana (✉)
Department of Chemistry, Osmania University, Hyderabad 500007, India
e-mail: ssnsirasani@gmail.com

N. Nambigari
Department of Chemistry, Nizam College, Osmania University, Hyderabad 500007, India

Introduction

During recent decades a variety of luminescent polypyridyl complexes employing a range of transition metal ions and ligands architectures have been reported. The luminescent and redox properties of Ru(II) and Co(III) complexes of 1, 10-phenanthroline (phen), 2, 2′ bipyridine(bpy), and related bidentate ligands have been studied due to their significant MLCT absorption in the visible region [1–3]. The clinical utility of transition metal complexes binding to DNA has inspired a great interest in the design and development of novel complexes that can be applied in DNA-structure probes, DNA "molecular light switches", DNA-photocleavage reagents, anticancer drugs and so forth [4–7]. In recent years, Ru(II) and Co(III) polypyridyl complexes have been employed in studies with DNA, with a view to design and develop synthetic restriction enzymes, new drugs and DNA footprinting agents [8–12]. The electron rich DNA bases, or phosphate groups are available for direct covalent coordination to a metal center. There are also non covalent binding modes, such as hydrogen bonding and electrostatic binding to grooved regions of the DNA and intercalation of planar aromatic ligands into the stacked base pairs. Varying substitutive group (or) substituent position in the intercalative ligands can create some interesting differences in the space configuration and electron density distribution of Ru(II) and Co(III) polypyridyl complexes. The ancillary ligands of Ru(II) and Co(III) polypyridyl complexes can have a significant effect on the spectral properties and the DNA binding behavior of the complexes [13, 14].

Recently, our group has been reported several polypyridyl ligand complexes of Ru(II) and Co(III) [15–27]. The aim of the present investigation is to study more in detail the effect of Ru(II) and Co(III) polypyridyl complexes with DNA. Herein, we report the synthesis and characterization of a new ligand

Published online: 11 March 2014

dmbip (2-(4-N, N-dimethylbenzenamine)1H-imidazo[4, 5-f][1, 10]phenanthroline) and its complexes $[Ru(phen)_2dmbip]^{2+}$ (1), $[Ru(bpy)_2dmbip]^{2+}$ (2), $[Co(phen)_2dmbip]^{3+}$ (3) and $[Co(bpy)_2dmbip]^{3+}$ (4) [where phen=1, 10-phenanthroline, bpy=2, 2′-bipyridine] (Fig. 1). The binding properties on Ru(II) and Co(III) complex to calf thymus DNA in physiological buffer (pH 7.4) was investigated by multi-spectroscopic methods. The results showed that spectroscopic techniques could provide a convenient way to characterize both the binding mode and the interaction mechanism of Ru(II) and Co(III) polypyridyl complex to DNA. All the four complexes were screened for Photo cleavage of pBR322 DNA and antimicrobial activity. The cytotoxicity of complexes 1, 2, 3 and 4 has been evaluated by MTT {MTT=(3-(4,5-dimethylthiazol-2-yl)-2,5diphenyltetrazolium bromide)} assay. We believe that the knowledge gained from this study will be helpful to further understand the binding mechanisms and can provide much fruitful information for designing a new type of highly effective anti tumor drugs.

Experimental

Physical Measurements

UV-Visible spectra were recorded with an Elico Bio-spectrophotometer, model BL 198. IR spectra were recorded in KBr discs on a Perkin-FT-IR-1605 spectrophotometer ^1H NMR and ^{13}C NMR spectra were measured on a Bruker Z-Gradient 400 MHz spectrophotometer using DMSO-d_6 as the solvent. Electrospray ionization mass spectrometry (ESI-MS) was recorded on a LQC system (Finnigan MAT, USA) using CH_3CN as mobile phase. Fluorescence spectra were recorded with SL 174 spectrofluorometer, Viscosity experiments were carried out on Ostwald Viscometer, immersed in thermo stated water bath maintained at 30±0.1 °C. CT-DNA samples approximately 200 base pairs in average length were prepared by sonication in order to minimize the complexities arising from DNA flexibility. Cyclic voltmeter was carried out on WonATech multichannel potentiostat/galvanostat (WMPG1000, Gyeonggi-do, Korea), the Patch dock server tool was used to perform docking calculations and molecular modeling studies were carried out using the Hyper Chem 7.5 software.

Materials and Methods

$RuCl_3$, $CoCl_2$, 1, 10-phenanthrolinemonohydrate 2, 2′-bipypridine and DNA, were purchased from Merck(India). 1, 10-phenanthroline-5, 6-dione was synthesized according to literature procedure [28]. Dimethyl sulfoxide (DMSO) and RPMI 1640 were purchased from Sigma Aldrich. Supercoiled pBR322 DNA was obtained from Bangalore Genie. Doubly distilled water was used for preparing various buffers. The DNA had a ratio of UV absorbance at 260 and 280 nm of 1.8–1.9:1, indicating that the DNA was sufficiently free from protein [29]. DNA concentration per nucleotide was determined by using a molar absorption coefficient [6,600 M^{-1} cm^{-1}] at 260 nm [30]. The perchlorate salts of metal cations (Cd^{2+}, Zn^{2+} and Fe^{2+}) and tetrabutylammonium salts of anions (F^-, Br^-, Cl^- and CH_3COO^-) purchased from commercial suppliers and used as throughout the experiment.

Synthesis of Ligand

The ligand was synthesized according to the procedure in the literature [31]. A mixture of phen-dione (0.53 g, 2.50 mM), N, N-Dimethylaminobenzaldehyde (0.675 g, 3.50 mM),

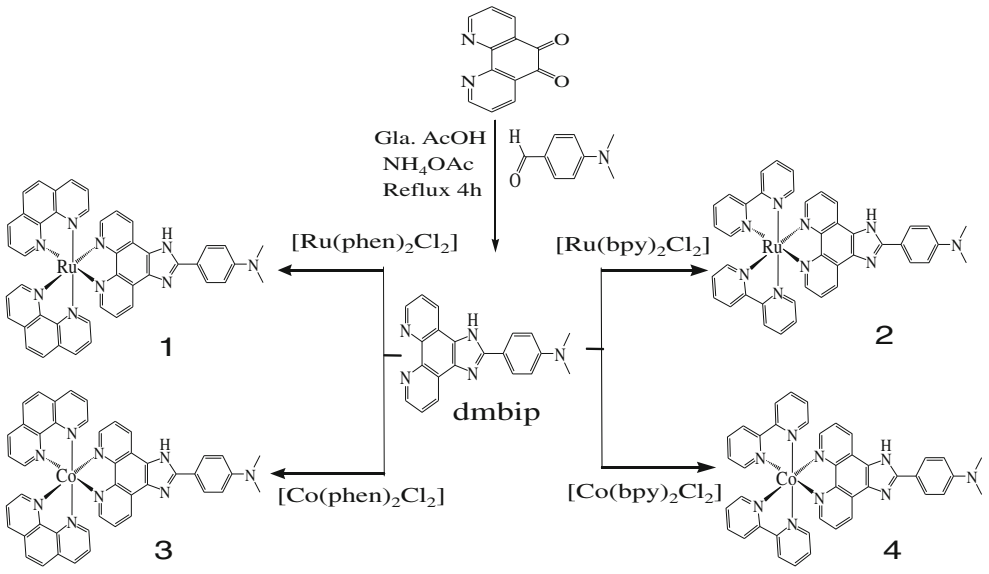

Fig. 1 Procedure for synthesis of ligand and complexes $[Ru(phen)_2(dmbip)]^{2+}$ (*1*), $[Ru(bpy)_2(dmbip)]^{3+}$ (*2*), $[Co(phen)_2(dmbip)]^{2+}$ (*3*) and $[Co(bpy)_2(dmbip)]^{3+}$ (*4*)

ammonium acetate (3.88 g, 50.0 mM) and glacial acetic acid (15 ml) was refluxed for 4 h. The above solution was cooled to room temperature and diluted with water, drop wise addition of Conc. NH_3 gave a yellow precipitate, which was collected, washed with H_2O and dried. The crude product recrystallized with C_5H_5N. H_2O and dried (yield: 71 %). Anal. data for $C_{21}H_{17}N_5$: calc. C, 74.32; H, 5.05; N, 20.63; found: C, 74.29; H, 5.01; N, 20.61. ES^+-MS Calc: 339; found: 340.

Synthesis of Complexes

[Ru(phen)$_2$(dmbip)](ClO$_4$)$_2$. 2H$_2$O

A mixture of $[Ru(phen)_2Cl_2]$ $2H_2O$ (0.531 g, 1.0 mM), dmbip (0.489 g, 1.5 mM) and ethanol (15 ml) was refluxed for 8 h under N_2 atmosphere. When the light purple color solution is obtained, it was cooled to room temperature and an equal volume of saturated aqueous $NaClO_4$ solution was added under vigorous stirring. The red solid was collected and washed with small amounts of water, ethanol and diethyl ether, then dried under vacuum (yield: 62 %). Anal. data for $RuC_{45}H_{37}N_9Cl_2O_{10}$: cal. C, 52.18; H, 3.60; N, 12.17; found: C, 52.14; H, 3.58; N, 12.11. ES^+-MS cal: 1035; found: 1036.

[Ru(bpy)$_2$(dmbip)](ClO$_4$)$_2$. 2H$_2$O

This complex was synthesized as described above by taking a mixture of $[Ru(bpy)_2Cl_2]$ $2H_2O$ (0.531 g, 1.0 mM), dmbip (0.489 g, 1.5 mM) (yield: 63 %). Anal. data for $RuC_{41}H_{37}N_9Cl_2O_{10}$: calc. C, 49.85; H, 3.78; N, 12.76; found: C, 49.81; H, 3.72; N, 12.71. ES^+-MS calc: 987; found: 988.

Table 1 ^{1}H NMR data of ligand and Ru(II) & Co(III) complexes

Compound	^{1}H NMR (400 MHz, ppm, DMSO-d$_6$, TMS)
dmbip	9.03(d, 2H); 8.95(d, 2H); 8.24(d, 2H); 7.21(d, 2H); 6.95(d, 2H); 2.10(s, 6H, –CH_3).
$[Ru(phen)_2(dmbip)]^{2+}$	9.16 (d, 6H), 8.71 (d, 6H), 8.26 (s, 4H), 8.11 (t, 6H), 7.77 (d, 2H), 6.84 (d, 2H), 2.76(s, 6H, –CH_3).
$[Ru(bpy)_2(dmbip)]^{2+}$	9.13 (d, 2H), 8.89(d, 4H), 8.83 (d, 4H), 8.23 (d, 2H), 8.12(t, 4H), 7.61(t, 2H), 7.35(t, 4H), 6.91(d, 2H) 6.74(d,2H), 2.78(s, 6H, –CH_3).
$[Co(phen)_2(dmbip)]^{3+}$	9.15(d, 6H), 8.60(d, 6H), 8.56(s, 4H), 7.98(t, 6H), 7.66(d, 2H), 6.78(d, 2H), 2.71(s, 6H, –CH_3).
$[Co(bpy)_2(dmbip)]^{3+}$	9.10(d, 2H); 8.79(d, 4H); 8.58(d, 4H); 8.21(d, 2H); 8.20(t, 4H); 7.50(t, 2H); 7.38(t, 4H); 6.87(d, 2H); 2.78(s, 6H, –CH_3).

Table 2 FT-IR data of Ru(II) & Co(III) complex

Compound	FTIR-data(Cm^{-1})			
	C=C	C=N	M-N(L)	M-N(dmbip)
dmbip	1,468	1,588	734	633
$[Ru(phen)_2(dmbip)]^{2+}$	1,460	1,581	728	629
$[Ru(bpy)_2(dmbip)]^{2+}$	1,603	1,445	722	623
$[Co(phen)_2(dmbip)]^{3+}$	1,541	1,430	714	624
$[Co(bpy)_2(dmbip)]^{3+}$	1,560	1,448	718	620

[Co(phen)$_2$(dmbip)](ClO$_4$)$_3$. 3H$_2$O

A mixture of $[Co(phen)_2Br_2]Br.$ $3H_2O$ (0.531 g, 1.0 mM), dmbip (0.489 g, 1.5 mM) in 50 ml ethanol was refluxed for 4 h to give a yellow solution. After filtration, the complexes were precipitated by addition of saturated ethanol solution of $NaClO_4$. The complex was filtered and further dried under vacuum before recrystallization (ethanol), (yield: 76 %) Anal. data for $CoC_{45}H_{39}N_9Cl_3O_{15}$: C, 48.64; H, 3.54; N, 11.35; found: C, 48.60; H, 3.51; N, 11.34. ES^+-MS: calc: 1109; found: 1110.

[Co(bpy)$_2$(dmbip)](ClO$_4$)$_3$. 3H$_2$O

This complex was synthesized as described above by taking a mixture of $[Co(bpy)_2Br_2]Br.$ $3H_2O$ (0.531 g, 1.0 mM), dmbip (0.489 g, 1.5 mM) (yield: 65 %) Anal. data for $CoC_{41}H_{39}N_9Cl_3O_{15}$: calc. C, 46.32; H, 3.70; N, 11.86; found: C, 46.30; H, 3.68; N, 11.82. ES^+-MS calc: 1061; found: 1062.

Spectroscopic Characterization

The IR spectral data for the complexes exhibit bands at 1,438 cm^{-1} and at 1,548–1,585 cm^{-1} due to C=C and C=N vibrations of the ring respectively. Bands were present around 567 cm^{-1} and 578 cm^{-1} corresponding to Co–N (phen) and Co–N of (bpy) respectively. In the ^{1}H NMR spectra of the

Table 3 $^{13}C[^1H]$-NMR data of Ru(II) & Co(III) complexes

Complex	^{13}C NMR (100 MHz, DMSO-d$_6$, major peaks)
$[Ru(phen)_2(dmbip)]^{2+}$	154.62, 153.16, 150.30, 147.83, 137.23, 130.92, 128.42, 126.25, 117.26, 112.52, 34.25.
$[Ru(bpy)_2(dmbip)]^{2+}$	157.43, 154.74, 152.04, 151.83, 149.91, 138.39, 130.99, 128.60, 128.23, 124.81, 117.36, 33.45.
$[Co(phen)_2(dmbip)]^{3+}$	155.53, 153.96, 146.22, 143.68, 136.15, 133.07, 131.75, 129.68, 129.11, 124.96, 116.53, 112.56, 33.53.
$[Co(bpy)_2(dmbip)]^{3+}$	152.82, 151.63, 150.79, 148.52, 146.35, 136.66, 130.45, 128.35, 126.51, 117.22, 112.36, 33.47.

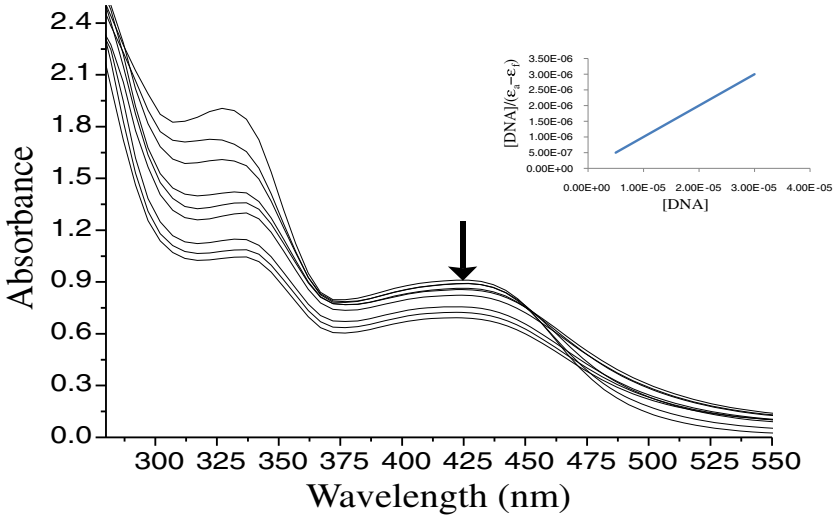

Fig. 2 Absorption spectra of $[Ru(phen)_2(dmbip)]^{2+}$ in tris-buffer in absence and presence of CT-DNA the [complex]=10–15 μM; [DNA]=0–126 μM. Insert plots of $[DNA]/(\varepsilon_a-\varepsilon_f)$ Vs [DNA] for the titration of DNA with complex. The *arrow* shows change in absorption with increasing DNA concentration

complexes the peaks due to various protons of ligand shifted downfield compared to the free ligand indicating complexation. As expected, the signals for the ligand appeared in the range around 7 to 9.8 ppm and the 6 hydrogens of the N-methyl group peaks appeared at 1.7–1.9 ppm, ^{13}C NMR peaks of the complexes appeared around 154.62 to 112.52 ppm and N-Methyl carbon peaks appeared around 34.25 to 33.53 (show in Tables 1, 2, and 3).

DNA Binding Studies

The interaction of Ru(II) and Co(III) complexes with DNA were studied in tris-buffer (5 mM Tris-HCl, 10 mM NaCl pH=7.1). The absorption titrations of these complexes were performed by treating fixed concentration of complexes (10 μM) with varying concentration (0–150 μM) of DNA. Complex-DNA solutions were allowed to incubate for 5 min before recording the absorption spectra. In order to evaluate the binding strength of the complex, the intrinsic binding constant K_b, with CT-DNA was obtained by monitoring the change in the absorbance at metal to ligand charge transfer (MLCT) band, with increasing concentration of DNA at 25 °C. The intrinsic binding constant K_b, was calculated from Eq. 1 [32].

$$[DNA]/(\varepsilon_a-\varepsilon_f) = [DNA]/(\varepsilon_b-\varepsilon_f) + 1/K_b(\varepsilon_b-\varepsilon_f) \quad (1)$$

where [DNA] is the concentration of DNA, ε_a, ε_f and ε_b corresponds to the apparent absorption coefficient A_{obsd}/[complex], the extinction coefficient for the free complex, and the extinction coefficient for the complex in the fully bound form, respectively. In plots of $[DNA]/(\varepsilon_a-\varepsilon_f)$ vs [DNA], K_b is given by the ratio of slope to the intercept.

In the emission studies fixed metal complex concentration (6 μM) was taken and to this varying concentration (0–150 μM) of DNA was added. The excitation wavelength was fixed and the emission range was adjusted before

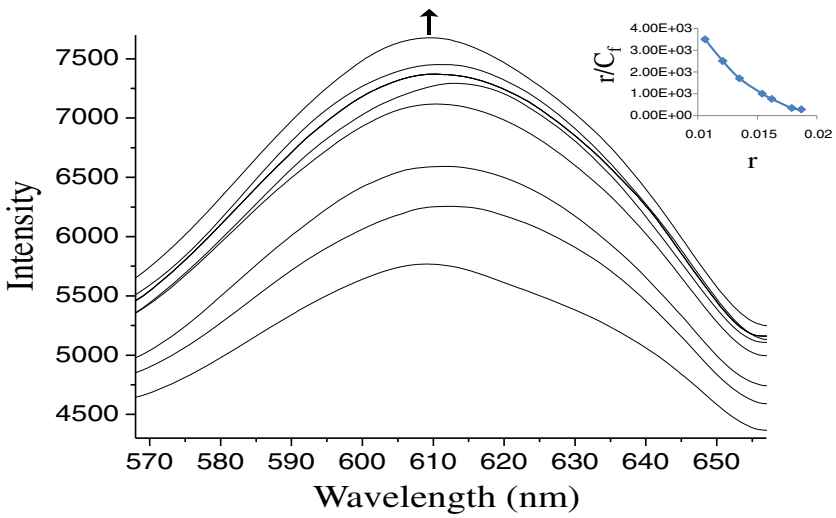

Fig. 3 Fluorescence spectra of $[Ru(phen)_2(dmbip)]^{2+}$complex in Tris-HCl buffer with increasing concentration of CT-DNA. The *arrow* shows the fluorescence intensity change upon increase of DNA concentration. *Inset*: Scatchard plot of r/C_f vs r

Table 4 Intrensic binding constants of absorption and emission studies of complexes

Complex	Hyperchromism (%)	Absorption Δ_λ	Absorption binding constant K_b	Emission constant
$[Ru(phen)_2(dmbip)]^{2+}$	21	14	2.2×10^5	7.3×10^5
$[Ru(bpy)_2(dmbip)]^{2+}$	18	11	1.3×10^5	5.5×10^5
$[Co(phen)_2(dmbip)]^{3+}$	19	9	1.7×10^5	7.1×10^5
$[Co(bpy)_2(dmbip)]^{3+}$	16	7	1.1×10^5	4.3×10^5

measurements. The fraction of the ligand bound was calculated from the relation $C_b = C_t[(F-F_0)/F_{max}-F_0)]$, where C_t is the total complex concentration, F is the observed fluorescence emission intensity at a given DNA concentration, F_0 is the intensity in the absence of DNA and F_{max} is the fully bound DNA to complex. Binding constant (K_b) was obtained from a modified Scatchard equation [33]. From a Scatchard plot of r/C_f vs r, where r is the C_b/[DNA] and C_f is the concentration of free complex.

Sensor studies were performed as follows, initially prepare stock solution of complexes in absolute CH_3CN dilute in tris-HCl buffer solution (10 mM; P^H=7.0). Aliquots of cations(Cd^{2+}, Zn^{2+}, and Fe^{2+}) and anions(F^-, Br^-, Cl^- and CH_3COO^-) were prepared in double distilled water. By taking the appropriate concentration of cations and anions injected to metal complexes, then observe change in emission spectra.

Viscosity experiments were carried out on Ostwald viscometer, immersed in thermo stated water bath maintained at 30±0.1 °C. CT-DNA samples approximately 200 base pairs in average length were prepared by sonication in order to minimize the complexes arising from DNA flexibility [34]. Data were presented as $(\eta/\eta_0)^{1/3}$ versus concentration of [Ru(II)]/[DNA], where η is the viscosity of DNA in the presence of the complex, and η_0 is the viscosity of DNA alone. Viscosity values were calculated from the observed flow time of DNA-containing solutions (t>100 s) corrected for the flow time of the buffer alone (t_0) [35].

Cyclic voltammogram recorded by using standard three electrode cell containing a platinum foil as working electrode, platinum wire as counter electrode and saturated calomel electrode (SCE) as reference electrode, 50 mg of the active compound (write your metal complex name instead of active compound) dissolved in 100 ml of acetonitrile containing 1 M Et_4NBF_4 at 10 mg/s scan rate.

For the gel electrophoresis experiments, Supercoiled pBR322 DNA (100 μM) was treated with Ru(II) complexes (40 and 80 μM) and the samples were irradiated at room temperature with a UV lamp (365 nm) for 30 min. The samples were analyzed by electrophoresis for 2.5 h at 40 V on a 0.8 % agarose gel in Tris-acetic acid-EDTA buffer. The gel was stained with 1 μg/ml ethidium bromide and then photographed under UV light.

Microbial activity was performed by the standard disc diffusion method [36]. The complexes were screened for

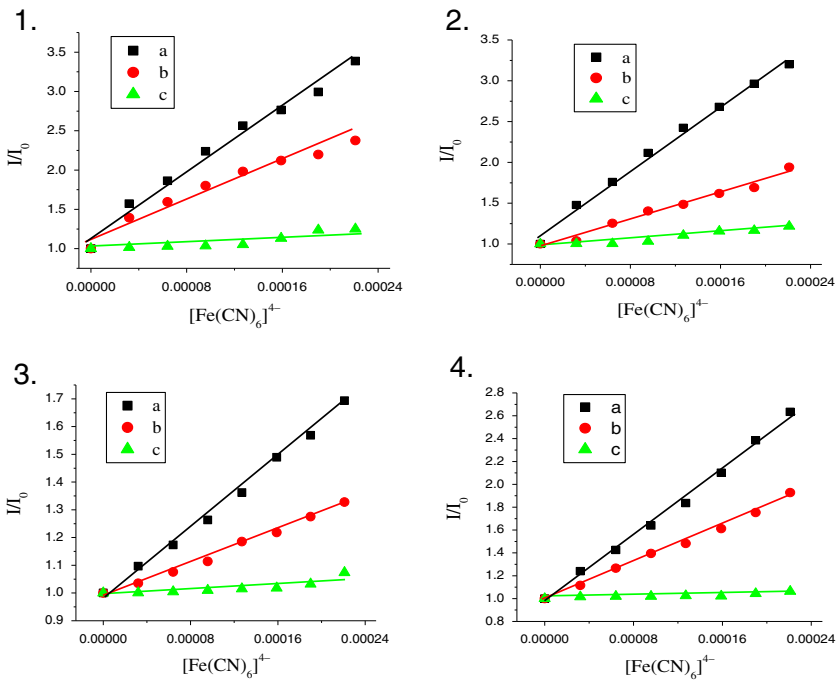

Fig. 4 Emission quenching of complexes $[Ru(phen)_2(dmbip)]^{2+}$ (**1**), $[Ru(bpy)_2(dmbip)]^{2+}$ (**2**) $[Co(phen)_2(dmbip)]^{3+}$ (**3**) and $[Co(bpy)_2(dmbip)]^{3+}$ (**4**) with $[Fe(CN)_6]^{4-}$in the absence of DNA (*a*), presence of DNA 1:30 (*b*) and 1:200 (*c*). [Ru] and [Co]= 10 μM, $[Fe(CN)_6]^{4-}$=0.1 M

antibacterial activity against standard microorganisms such as E. coli, Pseudomonas aeruginosa, Staphylococcus aurous and antifungal activity against Neurospora crassa, Aspergillusniger, Aspergillus flavus. The Mueller Hinton agar was prepared and poured fresh into sterile Petri plates and allowed to dry, and inoculate 0.2 ml of bacterial culture which has 106 cells/ml concentrations. The complex was dissolved in DMSO to get a final concentration of 100 μl per disc. Each plate contains standard microorganisms with three different complexes (5 μl each compound) and standard antibiotics were also tested on these standard microorganisms as controls, and kept in the refrigerator for 5 min and these were transferred to the incubator at 37 °C. After 24 h of incubation, the zone of inhibition of the complexes as well as standard antibiotics on standard microorganisms were checked. The minimum inhibitory concentrations for these complexes were measured.

Cytotoxicity was assessed using standard 3-(4, 5-dimethylthiazole)-2, 5-diphenyltetraazolium bromide (MTT) assay [37]. Cells were placed in 96-well microassay culture plates (8×10^3 cells per well) and grown overnight at 37 °C in a 5 % CO_2 incubator. The complexes tested were dissolved in DMSO and diluted with RPMI 1640 and then added to the wells to achieve final concentrations ranging from 10^{-6} to 10^{-4} M. Control wells were prepared by addition of culture medium (100 μL). The wells containing culture medium without cells were used as blanks. The plates were incubated at 37 °C in a 5 % CO_2 incubator for 48 h. Upon completion of the incubation, stock MTT dye solution (20 μL, 5 mg/ml) was added to each well. After 4 h, buffer (100 μL) containing N, N-dimethylformamide (50 %) and sodium dodecyl sulfate (20 %) was added to solubilize the MTT formazan. The optical density of each well was then measured on a microplate spectrophotometer at a wavelength of 490 nm. The IC_{50} values were determined by plotting the percentage viability against concentration on a bar graph and reading of the concentration at which 50 % of cells remain viable relative to the control. Each experiment was repeated at least three times to get the mean values. Hela and A549 cell lines were the subjects of this study.

Results and Discussion

Absorption Spectral Studies

The application of electronic absorption spectroscopy in DNA-binding studies are one of the most useful techniques. Complex binding with DNA through intercalation usually results in hypochromisum and bathochromisum, because of the intercalative mode involving a strong stacking interaction between an aromatic ligands and DNA base pairs. The absorption spectra of complex $[Ru(phen)_2dmbip]^{2+}$ in the absence and presence of CT-DNA is shown in Fig. 2. The bands below 300 nm are attributed to intraligand $\pi \rightarrow \pi^*$ transitions

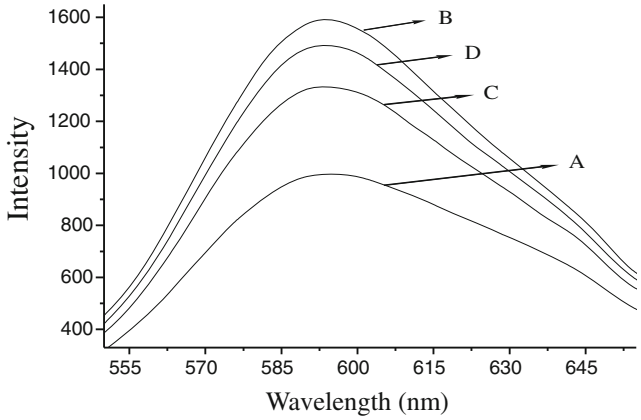

Fig. 5 The luminescence changes upon addition of Co^{2+}, EDTA to $[Ru(phen)_2dmbip]^{2+}$ + DNA. $[Ru(phen)_2dmbip]^{2+}$ complex alone (*A*), $[Ru(phen)_2dmbip]^{2+}$ + CT-DNA (*B*), $[Ru(phen)_2dmbip]^{2+}$ + DNA + Co^{2+} (*C*) and $[Ru(phen)_2dmbip]^{2+}$ + DNA + Co^{2+} + EDTA (*D*)

(1–4 complexes), while the metal to ligand charge transfer (MLCT) bands (metal dπ orbital to ligand π* orbital) appear at 447, 452, 318 and 327 nm, for complexes 1, 2, 3 and 4, respectively. The change in absorbance of the MLCT bands with increasing amount of CT-DNA was used to derive the intrinsic binding constants (K_b) [38, 39]. The values of K_b for complexes 1, 2, 3 and 4 are 2.2×10^5, 1.3×10^5, 1.7×10^5 and 1.1×10^5, respectively. Hence, the binding constants show the following order: $[Ru(phen)_2dmbip]^{2+}$ > $[Co(phen)_2dmbip]^{3+}$ > $[Ru(bpy)_2dmbip]^{2+}$ > $[Co(bpy)_2dmbip]^{3+}$. The complexes $[Ru(phen)_2dmbip]^{2+}$ and $[Co(phen)_2dmbip]^{3+}$ posses more binding constants than their respective bipyridyl complexes, because from bpy to phen planar area and hydrophobicity increase, which would lead to a greater binding affinity for DNA.

Fluorescence Spectroscopy

The fluorescence spectroscopy gives further clarification to investigate the interaction between complex and DNA. Figure 3

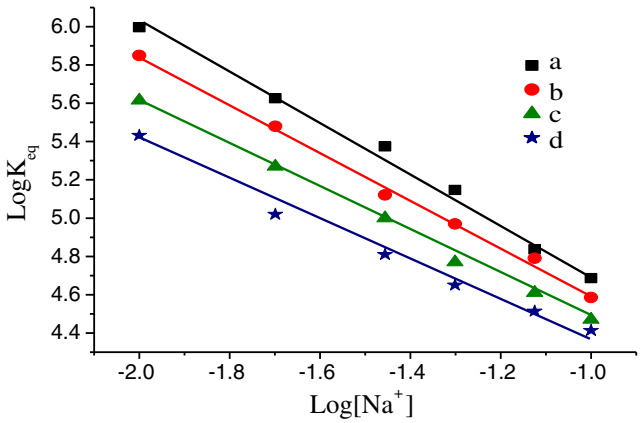

Fig. 6 Salt dependence studies of $[Ru(phen)_2(dmbip)]^{2+}$ (*a*), $[Co(phen)_2(dmbip)]^{3+}$ (*b*), $[Ru(bpy)_2(dmbip)]^{2+}$ (*c*) and $[Co(bpy)_2(dmbip)]^{3+}$ (*d*) complexes

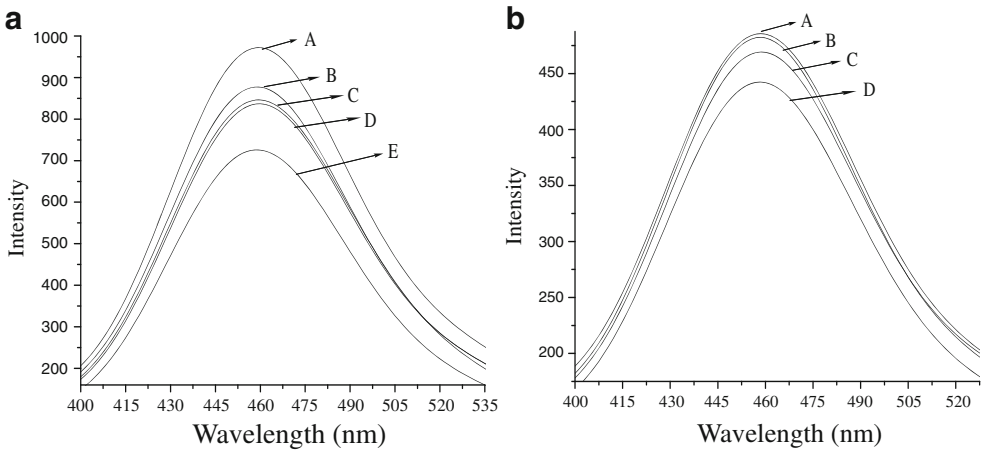

Fig. 7 **a** Anion sensor studies of $[Ru(phen)_2dmbip]^{2+}$ complex alone (*A*), $[Ru(phen)_2dmbip]^{2+}$ + Cl^- (*B*), $[Ru(phen)_2dmbip]^{2+}$ + Br^- (*C*), $[Ru(phen)_2dmbip]^{2+}$ + CH_3COO^- (*D*) and $[Ru(phen)_2dmbip]^{2+}$ + F^- (*E*). **b** Cation sensor studies of $[Ru(phen)_2dmbip]^{2+}$ complex alone (*A*), $[Ru(phen)_2dmbip]^{2+}$ + Cd^{2+} (*B*), $[Ru(phen)_2dmbip]^{2+}$ + Zn^{2+} (*C*) and $[Ru(phen)_2dmbip]^{2+}$ + Fe^{2+} (*D*)

showed the fluorescence spectra of $[Ru(phen)_2(dmbip)]^{2+}$ complex in the absence and in the presence of CT-DNA. The complexes 1, 2, 3 and 4 can emit fluorescence in Tris buffer at ambient temperature with a maximum appearing at 607, 610, 425 and 403 nm, respectively. The emission intensities of complexes 1, 2, 3 and 4 increased sharply and reach as high as 1.72, 1.65, 1.68 and 1.59 times of the original intensities, respectively. This implies the above four complexes can strongly interact with DNA and can be protected by DNA efficiently, because the hydrophobic environment inside the DNA helix reduces the accessibility of solvent water molecules to the complex and the complex mobility is restricted at the binding site, leading to decrease of the vibration mode of relaxation. The binding data (Table 4) were cast into the form of a Scatchard plot of r/C_f vs r, where 'r' is the binding ratio of C_b/[DNA] and C_f is the free ligand concentration. The binding constants are 7.3×10^5, 5.5×10^5, 7.1×10^5 and 4.3×10^5 for complexes 1, 2, 3 and 4, respectively.

Emission Quenching Studies

The quenching experiments may give further information about the binding ability of complex with DNA. In the absence of DNA, the emission of complexes were efficiently quenched by quencher $[Fe(CN)_6]^{4-}$. Emission quenching with $[Fe(CN)_6]^{4-}$ in the presence of DNA are shown in (Fig. 4) for four complexes. The Stern–Volmer quenching constant K_{sv}, can be determined by using Stern–Volmer equation [40].

$$I_0/I = 1 + K_{sv}[Q],$$

where I_0 and I are the emission intensities in the absence and presence of quencher $[Fe(CN)_6]^{4-}$, K_{sv} is the linear Stern–Volmer constant and [Q] is the quencher concentration. In the quenching plot of I_0/I Vs [Q], slope is the K_{sv}. The K_{sv} values for the complexes $[Ru(phen)_2dmbip]^{2+}$, $[Ru(bpy)_2dmbip]^{2+}$, $[Co(phen)_2dmbip]^{3+}$ and $[Co(bpy)_2dmbip]^{3+}$ in the absence of DNA were 32, 24, 30 and 23, respectively. In the presence of DNA, the K_{sv} values were 23, 17, 21 and 15, respectively. Hence the K_{sv} values are smaller in the presence of DNA. From Quenching studies, it is clear that the DNA binding ability of complexes follows the order $[Ru(phen)_2dmbip]^{2+}$ > $[Co(phen)_2dmbip]^{3+}$ > $[Ru(bpy)_2dmbip]^{2+}$ > $[Co(bpy)_2dmbip]^{3+}$. Such a trend is consistent with the observation in electronic absorption titrations.

Light Switch "On and Off" Experiment

Above studies show that the presence of CT–DNA varies the photoluminescence intensity of Ru(II) and Co(III) complexes. Photoluminescence intensity of complexes could be tuned by introduction of Co^{2+} ions. The addition of Co^{2+} (0.01 mM) to the $[Ru(phen)_2dmbip]^{2+}$ complex bound to

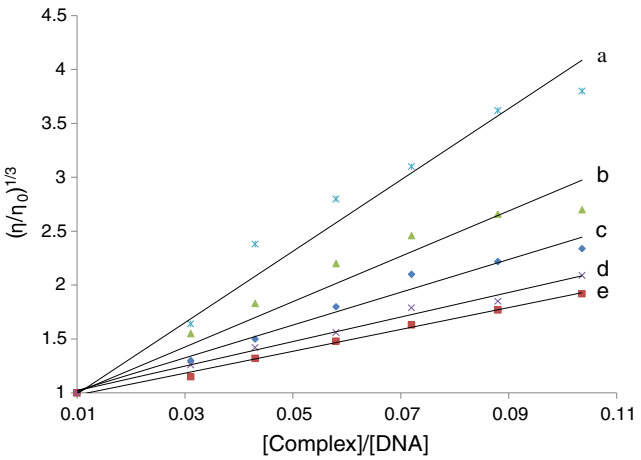

Fig. 8 Effect of increasing amounts of the Ru(II) and Co(III) complexes of *a*). Ethidium bromide, *b*). $[Ru(phen)_2(dmbip)]^{2+}$, *c*). $[Co(phen)_2(dmbip)]^{3+}$, *d*). $[Ru(bpy)_2(dmbip)]^{2+}$ and *e*). $[Co(bpy)_2(dmbip)]^{3+}$ complexes on the relative viscosity of CT-DNA at 27±0.1 °C

Table 5 Minimum inhibition concentration(MIC) of complexes and ligand (μg/ml) with Ecoli and S. aureus bacterias

S. no	Complex	E. coli (mM)			S. aureus (mM)		
		5 μl	10 μl	15 μl	5 μl	10 μl	15 μl
1.	dmbip (ligand)	2.0	2.2	2.5	2.0	2.1	2.6
2.	$[Ru(phen)_2dmbip]^{2+}$	4.0	6.0	8.0	4.5	7.0	8.2
3.	$[Ru\ (bpy)_2dmbip]^{2+}$	3.9	5.8	7.6	3.9	5.9	7.8
4.	$[Co(phen)_2dmbip]^{3+}$	2.8	5.9	7.4	2.9	6.0	7.7
5.	$[Co(bpy)_2dmbip]^{3+}$	2.8	5.8	7.3	2.7	5.9	7.6

DNA results in loss of luminescence due to the formation of Co^{2+}-$[Ru(phen)_2dmbip]^{2+}$. As shown in Fig. 5 when EDTA is added to the buffer system containing Co^{2+}-$[Ru(phen)_2dmbip]^{2+}$ the emission intensity of the complex is recovered again (light switch on) [41]. This indicates that the heterometallic complex (Co^{2+}-$[Ru(phen)_2dmbip]^{2+}$) becomes free again due to formation of EDTA-Co^{2+} complex. By repeating this titration with equimolar concentrations (0.01 mM) of Co^{2+} decreased the intensity of $[Ru(phen)_2dmbip]^{2+}$, and on adding equimolar concentrations (0.01 mM) EDTA photo luminescence recovered. Similar results are obtained for remaining complexes.

Salt-Dependent Studies

The polyelectrolyte theory quantitatively describes the thermodynamic linkage between cation and charged ligand binding to the DNA lattice. The dependency of the complex-DNA binding constant on cation concentrations is a manifestation of the thermodynamic linkage. As the concentration of salt (NaCl) increases, the binding constant decreases. From the polyelectrolyte theory, the slope of the lines in Fig. 6 provides an estimate of ZΨ. Where Ψ is the fraction of counter ions associated with each DNA phosphate (Ψ=0.88 for double-stranded B-form DNA) and Z is the charge on the complex. The data in Fig. 6 indicate that the data in Ru complexes carry a net charge of +2 and cobalt complexes carry a net charge +3. Consequently, the slopes of the lines are −1.363, –1.274, –1.171 and −1.142 for $[Ru(phen)_2dmbip]^{2+}$, $[Co(phen)_2dmbip]^{3+}$, $[Ru(bpy)_2dmbip]^{2+}$ and $[Co(bpy)_2dmbip]^{3+}$ complexes, respectively. These values are less than the theoretically expected value of ZΨ (Ru(II) 2×0.88=1.76 and Co(III) 3×0.88=2.64). Such lower values could arise from the coupled anion release (from the ligand) or from changes in ligand or DNA hydration upon binding. By increasing the Na^+ concentration, the knowledge of ZΨ allows for a quantitative estimation of the non electrostatic contribution to the DNA binding constant for the above four complexes [42].

Sensor Studies

Fluorescence spectroscopy studies were carried out in order to evaluate the ability of the receptors to operate as a fluorescent cation, and anion sensors. The emission spectrum of Ru(II) complex in CH_3CN showed a broad emission band at 460 nm. The effect of the anions (F^-, Br^-, Cl^- and CH_3COO^-) interacting with $[Ru(Phen)_2dmbip]^{2+}$ complex was investigated in CH_3CN. Figure 7a, showed that the addition of an excess of anions (F^-, Br^-, Cl^- and CH_3COO^-) as their tetrabutyl ammonium(TBA) salts to $[Ru(Phen)_2dmbip]^{2+}$ complex resulted in dramatic changes to the emission spectra; the addition of, Cl^- Br^- and CH_3COO^- anions slightly quenched the emission spectrum, whereas the addition of F^- anion was quite significant, giving rise to a large degree of quenching of the emission spectrum. Hence the order of quenching of anions to $[Ru(Phen)_2dmbip]^{2+}$ complex $Cl^- < Br^- < CH_3COO^- < F^-$. Similarly, the effect of the cations (Cd^{2+}, Zn^{2+} and Fe^{2+}) interacting with $[Ru(Phen)_2dmbip]^{2+}$ complex was investigated in CH_3CN. Figure 7b, showed that the addition of an excess of cations (Cd^{2+}, Zn^{2+} and Fe^{2+}) as their perchlorate salts to $[Ru(Phen)_2dmbip]^{2+}$ complex resulted in dramatic changes to the emission spectra, the addition of Cd^{2+} and Zn^{2+} slightly quenched the emission spectrum, whereas the addition of ferrous(Fe^{2+}) cation effectively quenched. Hence the order of quenching of cations to $[Ru(Phen)_2dmbip]^{2+}$ complex $Cd^{2+} < Zn^{2+} < Fe^{2+}$. It is clear the selectivity is an important characteristic of chemosensors, we have further evaluated the selectivity of $[Ru(Phen)_2dmbip]^{2+}$ complex for F^- (anion) and Fe^{2+} (cation) over the other anions and cations [43, 44].

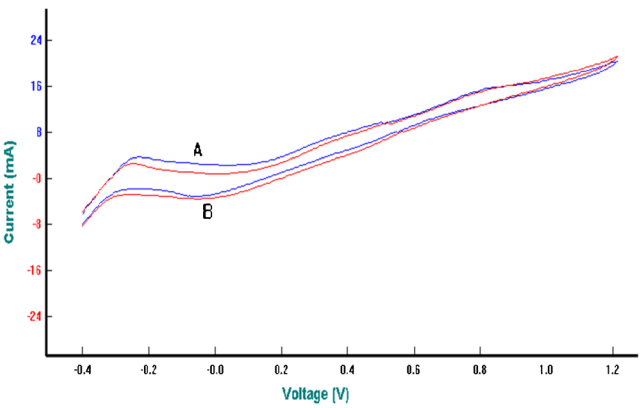

Fig. 9 Cyclic voltametry, *A* is $[Ru(phen)_2dmbip]^{2+}$ complex alone, *B* is $[Ru(phen)_2dmbip]^{2+}$ complex with CT-DNA

Viscosity Measurements

The viscosity studies provide a strong evidence for mode of binding. The viscosity measurements were carried out on CT–DNA by the addition of increasing of concentration of the complex. A classical intercalation model demands that the DNA helix lengthens as base pairs are separated to accommodate the bound ligand, which leads to an increase in the viscosity of DNA. In contrast, a partial, non-classical intercalation of ligand could bend (or kink) the DNA helix, reducing its length [45]. Viscosity of DNA in the presence of complexes 1, 2, 3, 4 and ethidium bromide (EB) are shown in Fig. 8. All

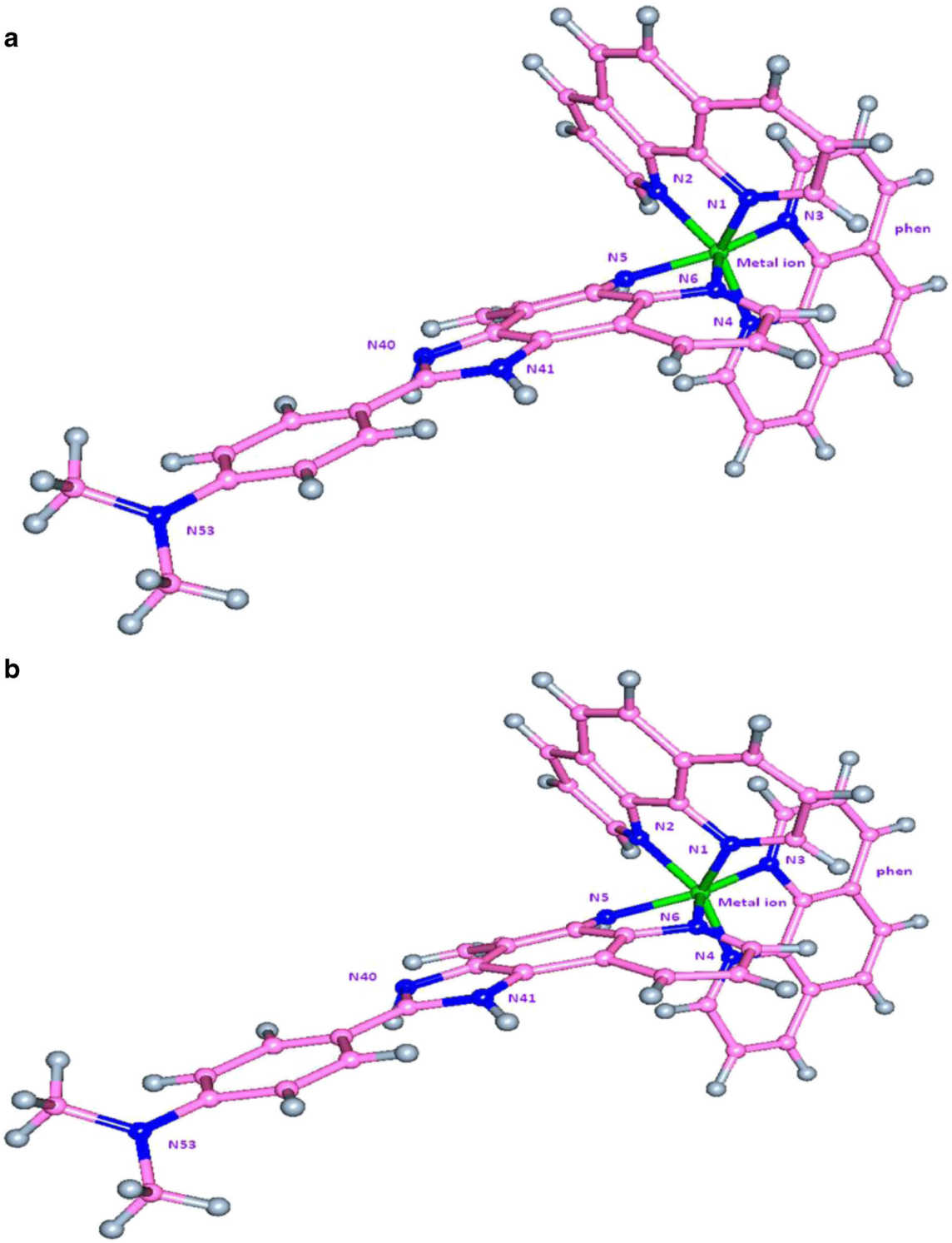

Fig. 10 Geometrically optimised model of the complex $[Ru(phen)_2dmbip]^{2+}$ (**a**); complex $[Co(phen)_2dmbip]^{3+}$ (**b**)

Table 6 Electrochemical behaviour of complexes alone and complexes with CT-DNA

Complex	Complex alone		Complex with CT-DNA	
	Anodoic (Epa)	Cathodoic (Epc)	Anodoic (Epa)	Cathodoic (Epc)
$[Ru(phen)_2dmbip]^{2+}$	0.23 V	−0.01 V	0.28 V	−0.09 V
$[Ru\ (bpy)_2dmbip]^{2+}$	0.21 V	−0.03 V	0.27 V	−0.07 V
$[Co(phen)_2dmbip]^{3+}$	0.19 V	−0.02 V	0.22 V	−0.035 V
$[Co(bpy)_2dmbip]^{3+}$	0.18 V	−0.025 V	0.21 V	−0.03 V

the four complexes of Ru(II) and Co(III) leads to increased relative viscosity of DNA. These results suggest that the complexes intercalate between the base pairs of DNA and the difference in the binding strength is probably caused by different ancillary ligands. Comparing bpy to phen, it is clear that the surface area and the hydrophobicity of ancillary ligand increase in phen, leading to a greater DNA binding affinity for complex 1. Thus, complex 1 is probably more deeply intercalated and more tightly bound to adjacent DNA base pairs than other complexes. Hence, follows the order EB>1>3>2>4.

Cyclic Voltammetry

The application of cyclic voltammetry (CV) to the study of binding of metal complexes to DNA provides a useful complement to the method for the investigation of UV-Vis spectroscopy and fluorescence spectroscopy. The interaction of DNA with $[Ru(phen)_2dmbip]^{2+}$ complex was characterized by the anodic peak current difference (ΔIpa) in cyclic voltammograms before and after addition of DNA to $[Ru(phen)_2dmbip]^{2+}$ complex in solution. Hence positive shift of peak potential indicates this interaction mode may be intercalation between $[Ru(phen)_2dmbip]^{2+}$ and DNA. The Ru(II) complex showing the anodic and cathodic peaks at 0.23 and −0.01 V respectively, after loading with DNA, the oxidation and reduction potentials are changed to 0.28 and −0.09 V which are shown in Fig. 9. Based on above oxidation and reduction potential shifting, it can be concluded that DNA binds to the Ru(II) complex through intercalation [46]. The decrease in current may be attributed to the diffusion of the complex bound to the large, slowly diffusing DNA molecule (Table 5). The decreases in the peak currents are ascribed to the stronger binding between Ru(II) and Co(III) complexes with DNA.

Table 8 Patch dock score and desolvation energies of the metal complex-DNA solution

S. no.	Complex	Patch dock score	−ACE[a]
1.	$[Ru(phen)_2dmbip]^{2+}$	5,350	−498.33
2.	$[Co(phen)_2dmbip]^{3+}$	5,222	−716.83
3.	$[Ru(bpy)_2dmbip]^{2+}$	5,438	−467.09
4.	$[Co(bpy)_2dmbip]^{3+}$	5,286	−478.22

[a] Desolvation energy

Molecular Modeling

Molecular modeling has become a vital technique in chemistry and challenging in the modeling of d and f-block complexes [47]. Molecular modeling studies were carried out

Table 7 Bond lengths of the 3D conformers of metal polypyridyl complexes

S. no.	Metal complex	Bond lengths (Å)					
		M-N1[a]	M-N2[a]	M-N3[a]	M-N4[a]	M-N5[b]	M-N6[b]
1.	$[Ru(phen)_2dmbip]^{2+}$	1.9508	1.9517	1.9476	1.9476	1.9471	1.9470
	Total energy	264.86 kcal/mol					
	Metal-intercalator length (Å)	12.8569					
2.	$[Co(phen)_2dmbip]^{3+}$	1.8683	1.8683	1.8692	1.8685	1.8677	1.8676
	Total energy	275.87 kcal/mol					
	Metal-intercalator length (Å)	12.7832					
3.	$[Ru(bpy)_2dmbip]^{2+}$	1.9507	1.9477	1.9435	1.9435	1.9476	1.9475
	Total energy	267.38 kcal/mol					
	Metal-intercalator length (Å)	12.8538					
4.	$[Co(bpy)_2dmbip]^{3+}$	1.9091	1.8364	1.8364	1.9082	1.9138	1.9396
	Total energy	313.71 kcal/mol					
	Metal-intercalator length (Å)	12.7920					

[a] N1, N2, N3 & N4 are Polypyridyl (phen/bpy) nitrogen bonded to metal
[b] N5 & N6, N of dmbip ligand bonded to metal

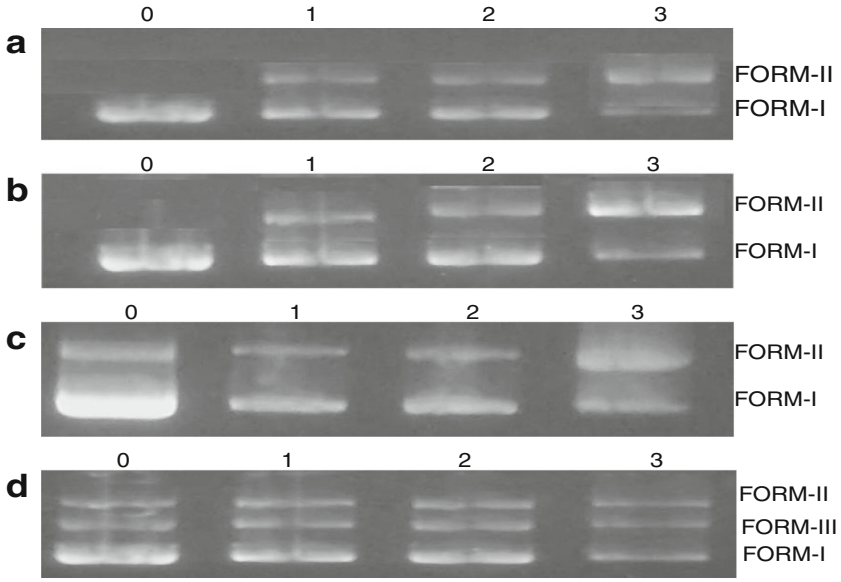

Fig. 11 Photocleavage studies of pBR322 DNA, in the absence and presence of complexes $[Ru(phen)_2(dmbip)]^{2+}$ (**a**), $[Co(phen)_2(dmbip)]^{3+}$ (**b**), $[Ru(bpy)_2(dmbip)]^{2+}$ (**c**) and $[Co(bpy)_2(dmbip)]^{3+}$ (**d**) after irradiation at 365 nm for 30 min. *Lane 0* was control (DNA alone), *lanes 1→3* were addition of complexes 20, 40 and 60 μM, respectively

using Hyper Chem 7.5 software [48]. The 3D structures of $[Ru(phen)_2dmbip]^{2+}$ (1), $[Ru(bpy)_2dmbip]^{2+}$ (2), $[Co(phen)_2dmbip]^{3+}$ (3) and $[Co(bpy)_2dmbip]^{3+}$ (4) complexes were built using drawing tools of the Hyper Chem model builder. Figure 10 shows 3D structures of $[Ru(phen)_2dmbip]^{2+}$ (1) and $[Co(phen)_2dmbip]^{3+}$ (3). The complexes were sketched individually in two dimensions (2D) and later converted into three dimensional (3D) entities using the conversion tool in the Hyper Chem Model Builder [49]. The 3D model built is subjected to a combination of optimization methods to search the potential energy matrix based on the contributions of a stretch, bending, dihedrals, Vander Waals and electrostatic interactions to the molecular energy (Eq. 2). A combination of optimization methods was used to search for the potential energy surface for energy minima.

$$E_{total} = E_{BL} + E_{DA} + E_{VDW} + E_{SBI} + E_{EE} \quad (2)$$

Table 9 Hydrogen bonding interactions involving the docked poses of dsDNA with metal complexes

S. no.	Complex	H-bond Donor group–acceptor group	Bond length (Å)	Vander Waals interactions (metal complex-DNA)	Bond length (Å)
1.	$[Ru(Phen)_2dmbip]^{2+}$	N53–ADG7: O3′	1.6493	N2–B DG22:O4′	3.0385
		N53–A DT8:OP1	2.2031	N2–B DG22:O3′	3.0031
		N53N–A DT8:OP2	0.9258	N45–A DC6: O3′	2.7403
		N53N–A DT8:O5′	1.9451	N45–A DG7: O5′	2.9141
2.	$[Co(Phen)_2dmbip]^{3+}$	N3–B DG22: O5′	2.3839	N3–B DG22 : O3′	3.0752
		N3–B DG23: O4′	1.8503	N4–B DG22 : O4′	2.7184
		N5–B DG22: O3′	2.0077	N6–B DG22: N3	2.9447
		N6–B DG22: O4′	1.5532		
		N40 : H1–B DC21: O4′	2.4976		
3.	$[Ru(Bpy)_2dmbip]^{2+}$	N41–A DG7:O3′	2.2589	N41–A DT8:OP1	2.9349
		N52–A DT8: O3′	1.5576	N41–A DT8: O5′	2.8412
		N52–A DC9: OP2	2.0410	N52–A DC9: OP1	2.7273
		N52–A DC9: O5′	1.3268	N52–ADC9: O4′	3.1606
4.	$[Co(Bpy)_2dmbip]^{3+}$	N3–A DA 5: O4′	2.1554	N3–A DA5: O4′	3.1374
		N3–ADA 5: O3′	2.4765	N4–A DC6 : OP1	3.0878
		N4–A DA5 : O3′	1.8565	N4–A DC6: O5′	3.0732
				N40–BDG23: O4′	3.2086
				N53–A DA5 : O3′	2.6779

Table 10 The IC_{50} values for complexes against A549 and HeLa cell lines

Compound	IC_{50} (μM)	
	A549	HeLa
$[Ru(phen)_2dmbip]^{2+}$	30	28
$[Ru\ (bpy)_2dmbip]^{2+}$	27	35
$[Co(phen)_2dmbip]^{3+}$	42	39
$[Co(bpy)_2dmbip]^{3+}$	46	52

The conjugate gradient method was chosen for the molecular mechanics calculation to obtain energy minima with the AMBER force field. Geometric optimization is carried out by Polak–Ribiere algorithm [50]. Unit final convergence criteria of 1×10^{-5} K.cal/mol per Å is obtained. Bond lengths of the 3D conformers of $[Ru(phen)_2dmbip]^{2+}$ (1), $[Ru(bpy)_2dmbip]^{2+}$ (2), $[Co(phen)_2dmbip]^{3+}$ (3) and $[Co(bpy)_2dmbip]^{3+}$ (4) complexes were reported in Table 6.

Docking Studies

Patch dock server tool was used to perform docking calculations between the metal complexes (ligand) and B–DNA (Receptor) sequence. Input used for the docking is the B–DNA sequence 5^1 –D(AP CP CP GP AP CP GP TP CP GP GP T)–3^1 which is obtained from Protein Data Bank (PDB id:423D) at a resolution of 1.6Å and the 3D models of the metal complexes built using Hyper Chem 7.5 are used. The receptor is prepared by deleting all the heteroatoms including water, Mg^{2+} ion and the polar hydrogen atoms were added. The PDB files of both DNA and metal complexes were uploaded. The program parameters were set to RMSD of 4Å and all other parameters were at default settings. Patch dock results were obtained as a set of scoring functions based on the shape complementarity and the ACE, the atomic desolvation energy of the transformed complex is evaluated. The ACE desolvation score is based on the sum of the ACE scores of all ligand atom-receptor atom pairs in contact. Patch Dock Score and Desolvation energies of four complexes-DNA solution were reported in Table 7 and Hydrogen bonding interactions involving the docked poses of ds-DNA with four complexes were reported in Table 8. The results have shown that all four complexes can bind to DNA through intercalative mode and complexes 1 and 3 are strong binding ability than 2 and 4.

Photocleavage of pBR322 DNA

After establishing the binding abilities of Ru(II) and Co(III) complexes with DNA, the photocleavage experiments were performed by agarose gel electrophoresis using plasmid DNA (pBR322 DNA) irradiated for 60 min at 302 nm. The pBR322 plasmid DNA can exist in three different forms supercoiled, nicked, and linear. These three different forms can be distinguished by gel electrophoresis. When circular plasmid DNA is subjected to electrophoresis, relatively fast migration will be observed in the intact supercoiled form (Form I) [51, 52]. If one strand is cleaved, the supercoil will relax to generate a slower moving open circular form (Form II). If both strands are cleaved, a linear form (Form III) that migrates between Form-I and Form-II will be generated. Figure 11 shows, no obvious DNA cleavage was observed for control (lane-0) in which complex was absent, or incubation of the plasmid with the complex in darkness, lanes 1→3 were added of complexes 20, 40 and 60 μM, respectively. With increasing concentration of Ru(II) and Co(III) complexes the amount of form-I pBR322 DNA was diminished gradually, whereas Form-II increases and Form-III is also produced.

Antimicrobial Studies of Ligand and Complexes

The antimicrobial screening data (Table 9) show that the $Ru(phen)_2dmbip]^{2+}$, $[Ru(bpy)_2dmbip]^{2+}$, $[Co(phen)_2dmbip]^{3+}$ and $[Co(bpy)_2dmbip]^{3+}$ complexes possess good antibacterial properties. Chelating tends to make the chelating ligands more potent bactereostatic agent, thus inhibiting the growth of bacteria upon complexation the lipophilic character increased and favours the permeation through the layer of the bacterial membranes. A zone of inhibition was

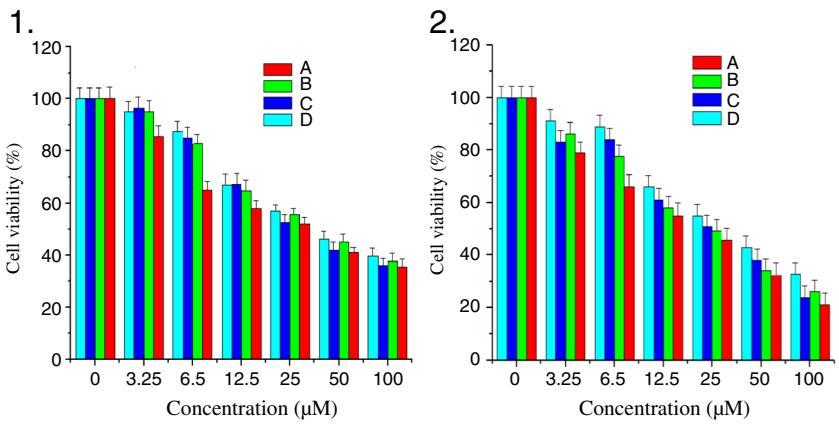

Fig. 12 Cell viability of cell lines HeLa (*1*) and A549 (*2*) in vitro after treatment with complexes $[Ru(phen)_2(dmbip)]^{2+}$ (*A*), $[Co(phen)_2(dmbip)]^{3+}$ (*B*), $[Ru(bpy)_2(dmbip)]^{2+}$ (*C*) and $[Co(bpy)_2(dmbip)]^{3+}$ (*D*)

measured for $Ru(phen)_2dmbip]^{2+}$, $[Ru(bpy)_2dmbip]^{2+}$, $[Co(phen)_2dmbip]^{3+}$ and $[Co(bpy)_2dmbip]^{3+}$ complexes as well as ligand against the bacteria *Escherichia coli (E. coli)* and *Staphylococcus aureus (S. aureus)* at 1 mg/ml concentration by the paper disc method using nutrient agar as the medium. DMSO control has negligible activity compared to the metal complexes. The complex 1 exhibited more antibacterial activity against both bacteria than other complexes and ligand. The antimicrobial activity increased as the concentration of the compounds increased. An increase in the lipophilic character of the complex favors its permeation through the lipid layer of the bacterial membrane, and therefore shows higher activity.

Cytotoxicity

The cytotoxicity assays of four complexes 1, 2, 3 and 4 against two kinds of tumor cells like A549 (Human alveolar adenocarcinoma cell line) and HeLa (Human cervical cancer cell line) at increasing concentrations for 48 h. The DMSO stock solution was used as a control for above four complexes to perform a proper comparison among the complexes and untreated cells. These four complexes are exhibited dose dependent growth inhibitory effect against the tested cell lines and IC_{50} (Inhibition of cell viability), values for all the complexes reported in Table 10. The above four complexes exhibited in vitro cytotoxicity against the selected cell lines. Figure 12 shows that the cell viability decreased with increasing concentration of complexes $[Ru(phen)_2dmbip]^{2+}$ (1), $[Ru(bpy)_2dmbip]^{2+}$ (2), $[Co(phen)_2dmbip]^{3+}$ (3) and $[Co(bpy)_2dmbip]^{3+}$ (4), respectively. Among the four complexes, the complex 1 is more effective than 2, 3 and 4 against both cell lines.

Conclusions

Ru(II) and Co(III) complexes have been synthesised, characterized and their interaction with CT-DNA were studied. From the absorption, fluorescence and viscosity experiments it is clear that the four complexes can intercalate into DNA base pairs via dmbip ligand. Ru(II) complexes bind to DNA strongly than Co(III) complexes because the size of Ruthenium metal is higher than cobalt metal. The difference in self aggregation and electronic effect induced by ruthenium metal. Ru(II) ion has 4d orbitals, these overlap strongly than Co(III) 3d orbitals with ligands. This makes intercalating ligand more electron deficient in Ru(II) complexes. The planarity of modified ligands plays an important role in DNA binding affinity. The complexes 1and 3 binds to DNA more strongly than 2 and 4 complexes, because 1 and 3 complexes have phenanthroline as ancillary ligand. Binding affinity follows the order 1>3>2>4. The experimental results show that Ru(II) and Co(III) complexes exhibited the DNA light switch on and off effect. In the cyclic voltammogram of Ru(II) and Co(III) polypyridyl complex the cathodic peak current decreased gradually with the addition of DNA, the decreases in the peak currents are ascribed to the stronger binding between the complex and DNA. Furthermore, the binding mode between the complexes and DNA was studied by molecular modeling and docking, the effects of the complexes on cell viability were tested using the MTT assay and results indicated that the four complexes had certain effect on cancer cells.

Acknowledgements We are grateful to DBT, New Delhi for financial support and CFRD, Osmania University, Hyderabad-07, for recording NMR spectra.

References

1. Brunschwig BS, Creutz C, Sutin N (1998) Electroabsorption spectroscopy of charge transfer states of transition metal complexes. Coord Chem Rev 177:61–79
2. Kober EM, Meyer TJ (1982) Concerning the absorption spectra of the ions M(bpy)t + (M = Fe, Ru, Os; bpy=2,2′-bipyridine). Inorg Chem 21:3967–3977
3. Kober EM, Marshall JC, Dressick WJ, Sullivan BP, Caspar JV, Meyer TJ (1985) Synthetic control of excited states. Nonchromophoric ligand variations in polypyridyl complexes of osmium(II). Inorg Chem 24:2755–2763
4. Barton JK (1986) Metals and DNA: molecular left-handed complements. Science 233:727–734
5. Norden B, Lincoln P, Akerman B, Tuite E (1996) DNA interaction with substitution-inert transition metal ion complexes. Met Ions Biol Syst 33:177
6. Ji LN, Zou XH, Liu JG (2001) Shape- and enantioselective interaction of Ru(II)/Co(III) polypyridyl complexes with DNA. Coord Chem Rev 216:513–536
7. Chen HL, Yang P, Yuan CX, Pu XH (2005) Study on the binding of base-mismatched oligonucleotide $d(GCGAGC)_2$ by cobalt(III) complexes. Eur J Inorg Chem 2005:3141–3148
8. Kane-Maguire NAP, Weeler JF (2001) Photoredox behavior and chiral discrimination of DNA bound $M(diimine)_3^{n+}$ complexes ($M = Ru^{2+}$, Cr^{3+}). Coord Chem Rev 211:145–162
9. Kaes C, Katz A, Hosseini MW (2000) Bipyridine: the most widely used ligand. A review of molecules comprising at least two 2,2′-bipyridine units. Chem Rev 100:3553–3590
10. Armitage B (1998) Photocleavage of nucleic acids. Chem Rev 98: 1171–1200
11. Sigman DS, Mazumdre A, Perrin DM (1993) Chemical nucleases. Chem Rev 93:2295–2316
12. De Armond MK, Carlin CM (1981) Multiple state emission and related phenomena in transition metal complexes. Coord Chem Rev 36:325–355
13. Xu H, Zheng KC, Deng H, Lin LJ, Zhang QL, Ji LN (2003) Effects of the ancillary ligands of polypyridyl ruthenium(II) complexes on the DNA-binding behaviors. New J Chem 27:1255–1263
14. Liu J-G, Zhang Q-L, Shi X-F, Ji L-N (2001) Interaction of $[Ru(dmp)_2(dppz)]^{2+}$ and $[Ru(dmb)_2(dppz)]^{2+}$ with DNA: effects of the ancillary ligands on the DNA-binding behaviors. Inorg Chem 40: 5045–5050
15. Yata PK, Shilpa M, Nagababu P, Reddy MR, Kotha LR, Gabra NM, Satyanarayana S (2012) Study of DNA light switch Ru(II)

complexes: synthesis, characterization, photocleavage and antimicrobial activity. J Fluoresc 22:835–847
16. Vidhisha S, Kotha LR, Ashwini Kumar K, Yata PK, Satyanarayana S (2010) DNA interactions of ruthenium (II) complexes with a polypyridyl ligand: 2-(2, 5dimethoxyphenyl)-1H-imidazo[4, 5-f] 1, 10-phenanthroline. Transit Met Chem 35:1027–1034
17. Shilpa M, Naveena Lavanya Latha J, Gayatri Devi A, Nagarjuna A, Kumar YP, Nagababu P, Satyanarayana S (2011) DNA-interactions of ruthenium(II) & cobalt(III) phenanthroline and bipyridine complexes with a planar aromatic ligand 2-(2-fluronyl)1H-imidazo[4,5-f][1,10-Phenanthroline]. J Incl Phenom Macrocycl Chem 70:187–195
18. Shobha Devi C, Anil Kumar D, Singh SS, Gabra NM, Deepika N, Yata PK, Satyanarayana S (2013) Synthesis, interaction with DNA, cytotoxicity, cell cycle arrest and apoptotic inducing properties of ruthenium(II) molecular "light switch" complexes. Eur J Med Chem 64:410–421
19. Deepika N, Yata PK, Shobha Devi C, Venkat Reddy P, Srishailam A, Satyanarayana S (2013) Synthesis, characterization, and DNA binding, photocleavage, cytotoxicity, cellular uptake, apoptosis and on–off light switching studies of Ru (II) mixed-ligand complexes containing 7-fluorodipyrido [3, 2-a: 2′, 3′-c] phenazine. J Biol Inorg Chem 18:751–766
20. Srishailam A, Yata PK, Gabra NM, Venkat Reddy P, Deepika N, Veerababu N, Satyanarayana S (2013) Synthesis, DNA-binding, cytotoxicity, photo cleavage, antimicrobial and docking studies of Ru(II) polypyridyl complexes. J Fluoresc 23:897–908
21. Gabra NM, Mustafa B, Yata PK, Shobha Devi C, Srishailam A, Venkat Reddy P, Kotha LR, Satyanarayana S (2013) Synthesis, characterization, DNA binding studies, photocleavage, cytotoxicity and docking studies of ruthenium(II) light switch complexes. J Fluoresc. doi:10.1007/s10895-013-1283-x (Accepted)
22. Ashwini KK, Kotha LR, Vidhisha S, Satyanarayana S (2009) Synthesis, characterization and DNA binding and photocleavage studies of $[Ru(bpy)_2BDPPZ]^{2+}$, $[Ru(dmb)_2BDPPZ]^{2+}$ and $[Ru(phen)_2BDPPZ]^{2+}$ complexes and their antimicrobial activity. Appl Organomet Chem 23:409–420
23. Kotha LR, Reddy YH, Kumar KA, Vidhisha S, Satyanarayana S (2009) Synthesis, characterization, DNA-binding, and DNA-photocleavage properties of $[Co(bpy)_2(7\text{-}NO_2\text{-}dppz)]^{3+}$, $[Co(dmb)_2(7\text{-}NO2\text{-}dppz)]^{3+}$, and $[Co(phen)_2(7\text{-}NO_2\text{-}dppz)]^{3+}$ complexes: (7-nitro-dppz=7-nitro dipyrido[3,2-a:2′-3′-c]phenazine; bpy=2,2′-bipyridine; dmb=4,4′-dimethyl-2,2′-bipyridine; phen=1,10-phenanthroline) and their toxicity on different microorganisms. Nucleosides Nucleotides Nucleic Acids 28:204–219
24. Nagababu P, Satyanarayana S (2007) DNA binding and cleavage properties of certain ethylenediamine cobalt(III) complexes of modified 1,10–phenanthrolines. Polyhedron 26:1686–1692
25. Nagababu P, Kumar DA, Reddy KL, Kumar KA, Mustafa MB, Shilpa M, Satyanarayana S (2008) DNA binding and photocleavage studies of cobalt(III) ethylenediamine pyridine complexes: $[Co(en)_2(py)_2]^{3+}$ and $[Co(en)_2(mepy)_2]^{3+}$. Metal Based Drugs 2008: 275084
26. Pallavi P, Nagababu P, Satyanarayana S (2007) Biomimetic model of coenzyme B_{12}: aquabis(ethane-1,2-diamine-κN, $\kappa N'$)ethylcobalt(III)—its kinetic and binding studies with imidazoles and amino acids and interactions with CT DNA. Helv Chim Acta 90:627–639
27. Shilpa M, Nagababu P, Kumar YP, Latha JN, Reddy MR, Karthikeyan KS, Gabra NM, Satyanarayana S (2011) Synthesis, characterization luminiscence studies and microbial activity of ethylenediamine ruthenium (II) complexes with dipyridophenazine ligands. J Fluoresc 21:1155–1164
28. Chaires JB, Dattagupta N, Crothers DM (1982) Self-association of daunomycin. Biochemistry 21:3927–3932
29. Satyanarayana S, Dabrowiak JC, Chaires JB (1993) Tris (phenanthroline) ruthenium(II) enantiomer interactions with DNA: mode and specificity of binding. Biochemistry 32:2573–2584
30. Barton JK, Danishefsky A, Raphael GJ (1984) Tris(phenanthroline) ruthenium)(II): stereoselectivity in binding to DNA. J Am Chem Soc 106:2172–2176
31. Ghosh BK, Chakravorty A (1989) Electrochemical studies of ruthenium compounds part I. Ligand oxidation levels. Coord Chem Rev 95:239–294
32. Wolfe A, Shimer GH Jr, Meehan T (1987) Polyclic aromatic hydrocarbons physically intercalate into duplex regions of denatured DNA. Biochemistry 26:6392–6396
33. McGhee JD, Von Hippel PH (1974) Theoretical aspects of DNA-protien interactions: co-operative and non-cooperative binding of large ligands to a one-dimensional homogeneous lattice. J Mol Biol 86:469–489
34. Chao H, Mei W-J, Huang Q-W, Ji L-N (2002) DNA binding studies of ruthenium(II) complexes containing asymmetric tridentate ligands. Inorg Chim Acta 357:285–293
35. Satyanarayana S, Dabrowiak JC, Chairs JB (1983) Tris(phenanthroline) ruthenium(II) enatiomer interactions with DNA: mode and specificity of binding. Biochemistry 32:2573–2584
36. Drew WL, Barry AL, Toole RO, Shreeis JC (1972) Reliability of the Kirby-Bauer Disc diffusion method for detecting methicillin resistant strains of Staphylococcus aureus. Appl Microbiol Am Soc Microbiol 24:240
37. Tselepi-Kalouli E, Katsaros N (1989) The interaction of $[Ru(NH_3)_5Cl]^{2+}$ and $[Ru(NH3)_6]^{3+}$ ions with DNA. J Inorg Biochem 37:271–282
38. Pyle AM, Rehmann PJ, Meshoyrer MR, Kumar CV, Turro NJ, Barton JK (1989) Mixed-ligand complexes of ruthenium(II): factors governing binding to DNA. J Am Chem Soc 111:3051–3058
39. Haga MA (1983) Synthesis and protonation–deprotonation reactions of ruthenium(II) complexes containing 2, 2′-bibenzimidazole and related ligands. Inorg Chim Acta 75:29
40. Joseph R, Lakowicz GW (1973) Quenching of fluorescence by oxygen. Probe for structural fluctuations in macromolecules. Biochemistry 12:4161–4170
41. Chen M, Li H, Li Q, Xu Z (2010) Luminescence properties of $[Ru(bpy)_2MDHIP]^{2+}$ modulated by the introduction of DNA, copper(II) ion and EDTA. Spectrochim Acta A Mol Biomol Spectrosc 75:1566–1570
42. Record MT Jr, Anderson CF, Lohman TM (1978) Thermodynamic analysis of ion effects on the binding and conformational equilibria of proteins and nucleic acids: the roles of ion association or release, screening, and ion effects on water activity. Q Rev Biophys 11:103–178
43. Gale PA (2011) Anion receptor chemistry. Chem Commun (Camb) 47:82–86
44. Jonathan AK, Elaine MB, Thorfinnur G (2012) Synthesis, structural characterisation and luminescent anion sensing studies of a Ru(II)polypyridyl complex featuring an aryl urea derivatised 2,2′-bpy auxiliary ligand. Inorg Chim Acta 381:236–242
45. Satyanarayana S, Dabrowiak JC, Chairs JB (1992) Neither Δ- nor Δ-tris(phenanthroline(ruthenium)(II) binds to DNA by classical interaction. Biochemistry 31:9319–9324
46. Li G, Liu N, Liu S, Zhang S (2008) Electrochemical biosensor based on the interaction between copper(II) complex with 4,5-diazafluorene-9-one and bromine ligands and deoxyribonucleic acid. Electrochim Acta 53:2870–2876
47. Cundari TR (1998) Molecular modeling of d- and f-block metal complexes. J Chem Soc Dalton Trans. doi:10.1039/A802144I
48. Rahman A, Amri, Sudrajat H, Maria TF, Erhard C (2009) Study on the conformations of P-(nitro)methoxycalix[4]arene and P-(tert-butyl) methoxycalix[4] arene using high level ab initio method. World J Chem 4:52–57

49. Tajmair-Riahi HA (2005) AZT binding to DNA and RNA: molecular modeling and biological significance. J Iran Chem Soc 2: 78–84
50. Grippo AL, Lucidi S (1997) A globally convergent version of the Polak-Ribiere conjugate gradient method. Math Program 78(3): 375–391
51. Basile LA, Barton JK (1987) Design of a double-stranded DNA cleaving agent with two polyamine metal-binding arms: $Ru(DIP)_2$macron. J Am Chem Soc 109:7548–7550
52. Kishikawa H, Jiang YP, Goodismam J, Dabrowiak JC (1991) Coupled kinetic analysis of cleavage of DNA by esperamicin and calicheamicin. J Am Chem Soc 113:5434–5440